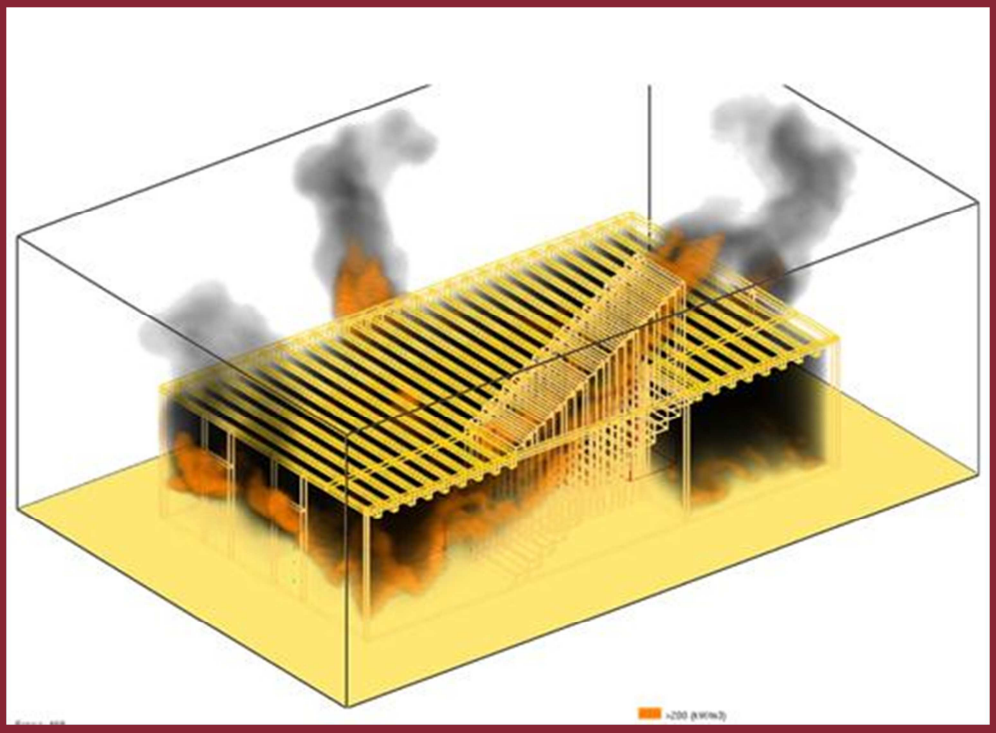

Fire Modeling of Basement with Wood Ceiling

Mahmood Tabaddor, PhD
Manager, Predictive Modeling and Risk Analysis Group
Corporate Research

DECEMBER 2011

Underwriters Laboratories Inc.
333 Pfingsten Road, Northbrook, IL 60062-2096 USA
T: 847.272.8800/W: UL.com

DOCUMENT INFORMATION

Release Type	☐ Internal ☐ External (Confidential) ☒ External (Public)	
UL Distribution	Corporate Research	
External Distribution	National Institute of Standards and Technology, www.ul.com	
Date: December 2011	**Keywords:** Fire Modeling, Wood, Basement, Ventilation	
Title: : Fire Modeling of Basement with Wood Ceiling		
Author(s)	**Department**	**Email**
Mahmood Tabaddor	Corporate Research - UL	Mahmood.tabaddor@ul.com
Reviewer(s)	**Department**	**Email**
Pravinray D. Gandhi	Corporate Research - UL	

ACKNOWLEDGEMENTS

UL would like to acknowledge the help of our partner, ESI-Mindware, in supporting the finite element analysis. We would like to thank the National Institute of Standards and Technology (NIST) for funding this work through the 2009 ARRA grant.

EXECUTIVE SUMMARY

A study on the fire dynamics within a large compartment with openings using the computational fluid dynamics based software, FDS v5, was carried out. The objective was to assess and help advance the predictive capabilities of FDS. The challenges for this particular scenario, in addition to those associated with general fire dynamics modeling within a compartment, where tied to the ceiling. The entire ceiling incorporated wood floor and support beams along with some geometric complexity.

The particular setup that was modeled was taken from one of several experiments conducted on basement fires with engineered wood I-beam ceilings as part of the overall research program (Kerber & et al., 2011). Figure 1 shows the details of the basement that were captured in the model. In this scenario, a heat source placed within the basement was ignited and the flames eventually reached the ceiling causing further ignition of the wood, continuing the spread of flame and heat.

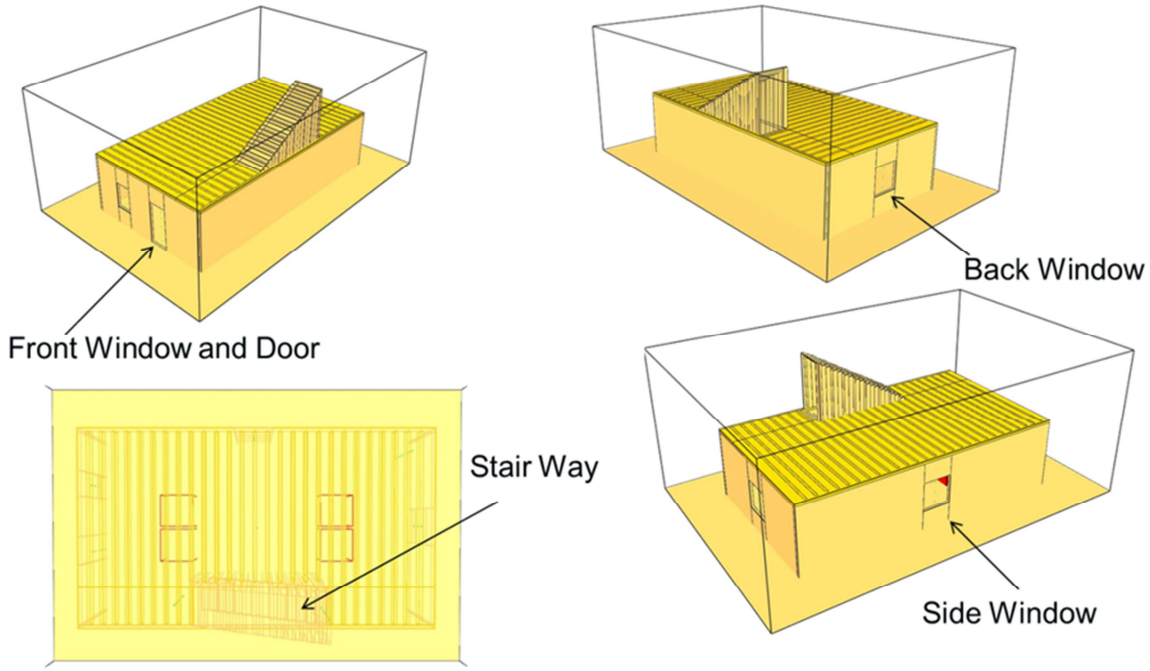

Figure 1

The basement model generated results both at discrete points and within planes related to temperature (both thermocouple and gas) and gas velocity along with flame and smoke visualization. Figure 2 shows a comparison of the flame and smoke visualization from the test and the model.

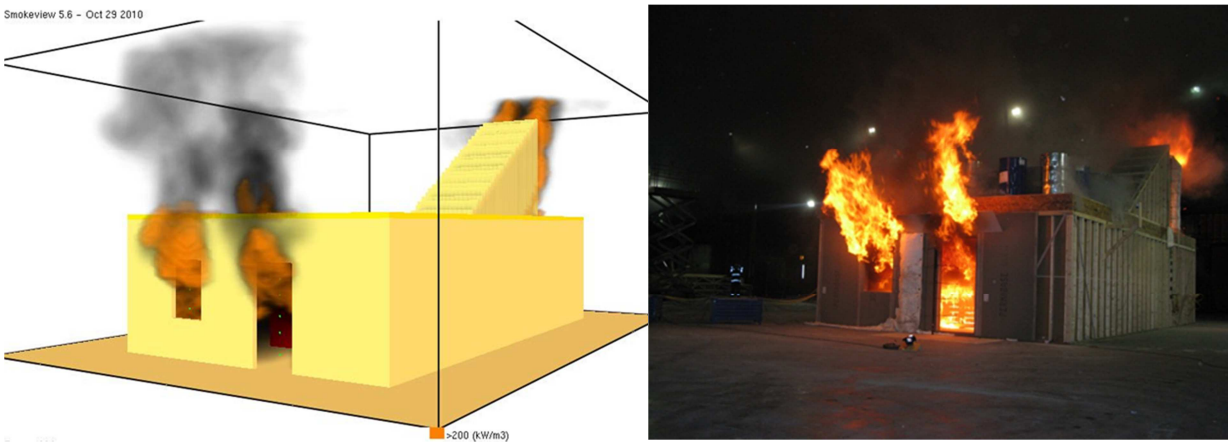

Figure 2

In general the model provided good agreement with bulk temperatures within the interior with differences noted at openings. Improvements in the predictability of the model can be tied to better heat release rate representation of the heat source and the burning wood.

Looking at some of the details of the model prediction, Figure 3 shows a snapshot of the gas temperature contours in plane cutting through the middle of the stairway. As the flames and hot air spread along the ceiling, they naturally followed the narrow channel created by the parallel engineered wood joists supporting the floor. Unlike the other door on the ground floor, the door for the stairway on the first floor was mostly seeing hot air leaving. Clearly, for an occupant to exit through the stairway would be hazardous.

In the fire tests, the engineered wood I-beams are constructed with thin webs which burn out during the test. This feature is not available with FDS yet as the solid thermal conduction is simply 1-D with no thermal communication between surfaces of the same obstruction. As the web burns and through holes are created both heat and flames travel more easily.

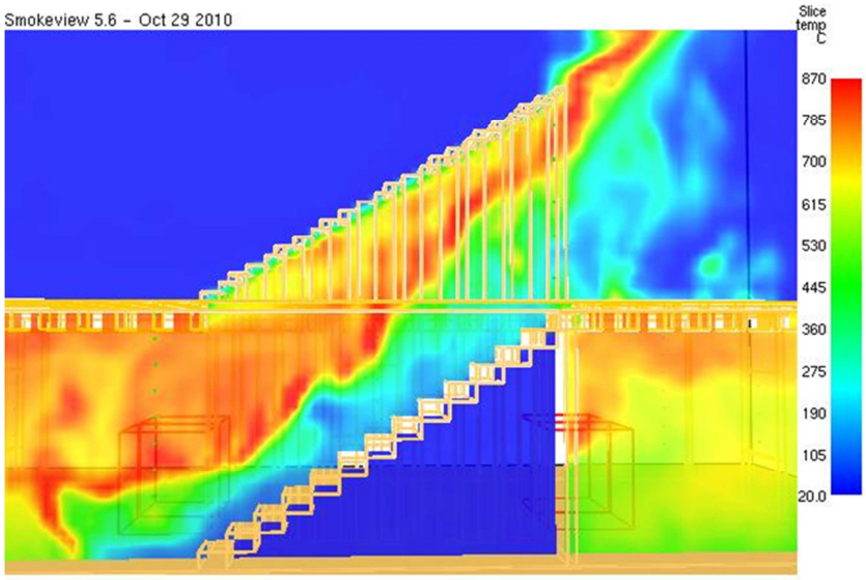

Figure 3

In the model heat and flames spread either by travelling along the narrow channel created by two adjacent joists (Figure 4) or over a joist in a lateral direction. The flow between the channels also is not adequately captured with only a few cells in a LES-based turbulent simulation.

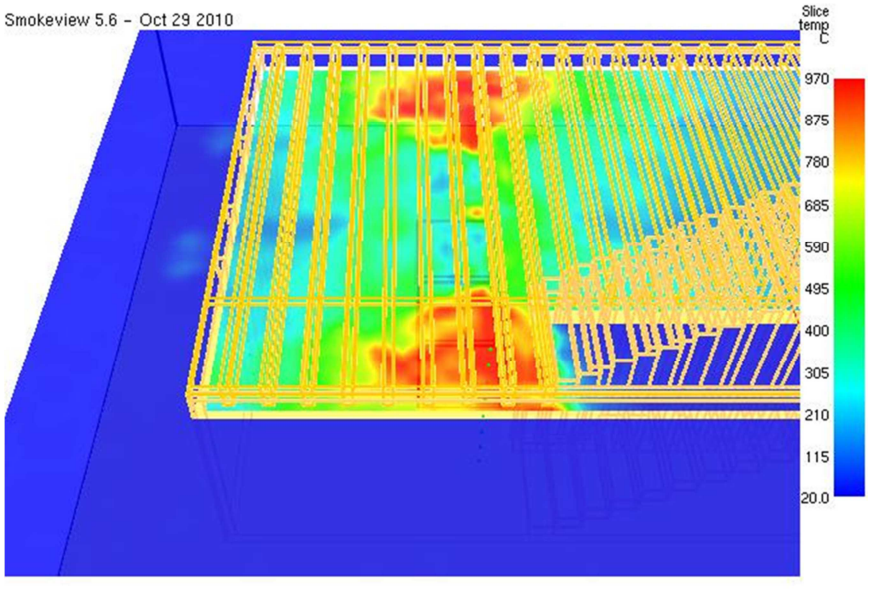

Figure 4

All these shortcomings aside, the FDS model of a compartment fire with a combustible ceiling displaying some geometric complexity appears to provide an acceptable level of modeling. The continuation of this work towards investigating the alteration of basement factors would help further confirm the conclusions of this research and possibly provide a new set of benchmark studies.

TABLE OF CONTENTS

INTRODUCTION

Progress in the field of fire safety is highly dependent upon advances in and application of high performance computing (HPC) tools in simulating the behavior of fire and the other products of combustion in buildings. The economic challenges of large-scale fire testing and the technical challenges of extrapolating large-scale fire behavior from small-scale tests will remain. Also physical experiments suffer constraints on the type of physical parameters that can be measured and that too at discrete points. On the other hand HPC based simulation, or virtual testing, is data rich. Simulation can generate data throughout the computational domain allowing for understanding of global and local energy conversions and flows. Only this type of comprehensive data coupled with strong visualization tools can give insights necessary for understanding complex phenomenon such as fire. However, the key step in advancing fire modeling tools is validation and validation cannot be carried out without well-designed and executed experiments. For this reason, the design of fire tests must also consider the requirements necessary for model validation.

For building designers and safety officials, the ability to address fire safety still relies mainly on a prescriptive approach or simplified engineering analysis. However, a full building fire risk analysis would require consideration of details that affect fire initiation and the spread and growth of fire and other products of combustion (Yung, 2008). The ability to model compartment fire spread/growth and products of combustion will provide fire safety engineers and building designers a tool to move beyond prescriptive methods and consider details such as effectiveness of detection systems and human egress. Without such tools, it is difficult to map the fire risks of buildings with complex and irregular architecture and the myriad of dynamic conditions such as ventilation and varying fuel load. The benefits of modeling are not limited to the engineer and designer but will certainly help firefighters update and customize tactics (Eliasson & al., 2008).

The purpose of this research is to help assess and advance the state of art in computational fluid dynamics (CFD) modeling of compartment fires. In this research, the compartment represents a residential basement with an unprotected engineered wood ceiling under load and with a variety of openings (Kerber & et al., 2011). Only a single CFD code, Fire Dynamics Simulator (FDS) developed by National Institutes for Standards and Technology (NIST), was employed as this is freeware popular amongst the fire engineering community (McGrattan & et al., 2010). The strengths of FDS versus

other CFD codes are its relatively easy setup, its focus on key physical mechanisms and solvers important for fire modeling reducing user effort, and a powerful visualization tool.

Brief Survey of Research[1]

Most modeling of compartment fires concerns the evolution of the hot gas layer, transition to flashover, and the movement of smoke and other products of combustion under a particular fuel load within a compartment with openings (Karlsson & et al., 2000). The fire modeling of compartment fires can simulate a variety of fire scenarios: naval ships (Floyd & et al., 2005), subway tunnels (Kayili, 2005), mines (Prosser & et al., 2010), offices (Chen & et al., 2010), residential buildings (Lin & et al., 2006) and nuclear plants (Dey, 2009) (Stroup & et al., 2011).

The fire growth and smoke spread within a building – a series of connected compartments – involves numerous factors (Figure 5). Any single fire test, unless for a specific configuration and condition of interest, will not help advance general understanding of building safety without a large number of tests to cover the large number of factors. However, a more systematic approach that combines tests designed to provide both insight and data for fire model validation will help advance both understanding of safety risks and applicability of such tools more efficiently (Coyle & et al., 2007).

Aside from CFD-based fire modeling, there are other engineering methods that are used and Table 1 describes the different methods ranging from simplified equations for hand calculations to zone models to CFD based fire models for fires in a single compartment. These non-CFD based models were formulated through analysis of fire tests and first order principles and certainly play an important role for engineers. They provide quick order of magnitude estimates for some simple situations without much detail but cannot handle complex multi-compartment configurations. Though, not common, an analysis of a multitude of simulation results from CFD based fire models could also be used to generate simplified equations for certain conditions which can help the engineer carryout analyses more quickly. This could allow for an efficient tiered approach using a variety of engineering tools.

[1] This section provides only a sampling of research that was found through Google search for articles and reports written in English mostly since 2004.

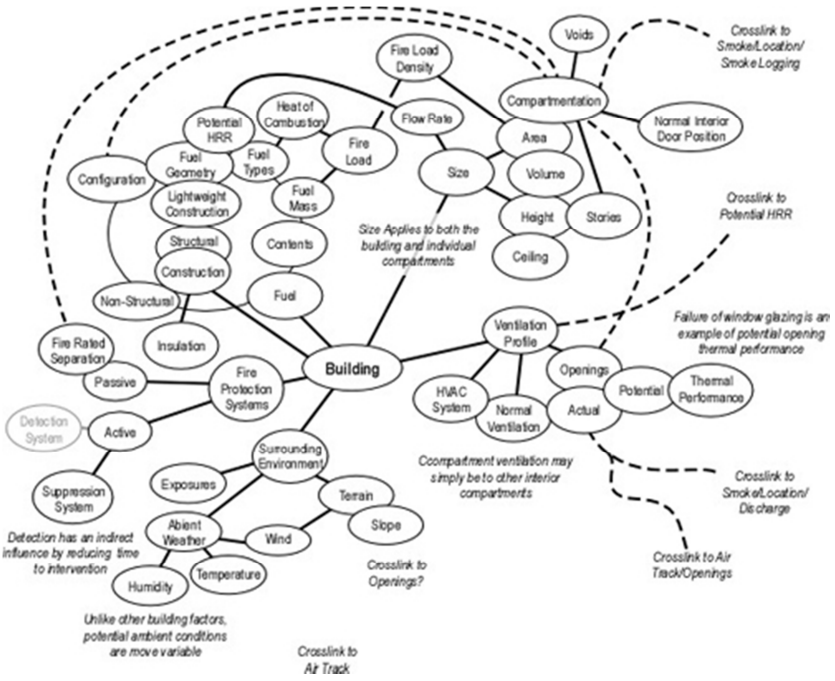

Figure 5 Concept Map for Building Factors Affecting Fire Safety (Hartin, 2009)

When the engineer must predict fire growth and smoke spread through multiple compartments, then a network model approach may be used (Floyd & et al., 2005) as an alternative to CFD modeling. A network fire model represents a compartment (or control volume) as a node. Ventilation effects are captured through node to node connections. However, compartments are represented by single quantities (temperature, etc.). CFD based fire modeling tools do not have these constraints and will be the key tool in advancing fire engineering from a prescriptive to a performance basis (Novozhilov, 2001).

With CFD based fire models, detailed data for a large number of variables is available throughout the computational domain. For instance, it can be shown that in some cases a great deal of thermal energy accumulates within the walls and so transient processes are affected by the level of wall modeling (Liu & et al., 2004). For modeling fires in compartments, the key physical processes that must be modeled include heat transfer due to radiation, buoyancy driven flow, combustion, and turbulence. In particular, the emergence of large eddy simulation in turbulence modeling is driven by fire modeling. Though, the modeling of turbulence is still very challenging and known to be highly sensitive to grid resolution (Gant, 2010). For example, Ryder and colleagues (Ryder & et al.,

2004) found that a coarse grid can lead to over-prediction of mean velocity and temperature. However, often engineers cannot refine a model mesh sufficiently due to either constraint on computational time or computer hardware limitations.

Table 1 Methods for modeling compartment fires (IStructE, 2007)

Fire model	Nominal fires	Time equivalence	Natural fire curves	Localised fires	Zone models		CFD/field models
					One-zone	Two-zone	
Complexity	Simple	Intermediate			Advanced		
Fire behaviour	Post-flashover fires			Pre-flashover fires	Post-flashover fires	Pre-flashover/ localised fires	Complete temperature-time relationships
Temperature distribution	Uniform in whole compartment			Non-uniform along plume	Uniform	Uniform in each layer	Time and space dependent
Input parameters	• Constant time-temp. relationship • No physical parameters	• Fire load • Ventilation conditions • Thermal properties of boundary • Compartment size		• Fire load and size • Height of ceiling	• Fire load • Ventilation conditions • Thermal properties of boundary • Compartment size • Detailed input for heat and mass balance of the system		Detailed input for solving the fundamental equations of the fluid flow
Design tools	Simple equations for hand calculations		Spread-sheet	Simple equations	Computer models		

For compartment fires, the hot gas layer generated by the fire source rises and impacts the ceiling, causing both heat and smoke to travel along the ceiling. If there is mechanical ventilation nearby or a sudden change in ventilation (such as broken window), the fire dynamics will be altered. The enclosure dimensions and available ventilation mainly affect radiation heat transfer and oxygen availability. Even in an enclosed compartment, leakage is present which may influence fire dynamics. Another concern is the transport of un-burnt gases which might mix with oxygen near openings causing flames to appear. In some cases when the fuel source is a liquid, ghosting flames are observed depending upon the combustion regime and ventilation state (Guigay & al., 2006).

One area that has contributed to the growth of CFD modeling of building fires is forensic studies. In these cases, well publicized but little understood actual fire incidents are modeled in an attempt to gain insight into ignition, fire/smoke growth and spread with the possibility of updating codes and

practices to improve fire safety in buildings. One important example is the fire modeling carried out by NIST on the 2001 collapse of the World Trade Center buildings in New York City (McGrattan & et al., 2005). The model using FDS was used to predict temperature buildup and fire spread. Results from the model were provided as inputs to compute the resulting structural responses.

Other research on fire modeling within confined spaces involves simulating fire spread and smoke growth in an effort to predict the performance of detection devices (Saunders, 2010) and suppression systems (Tabaddor & et al., 2011). Finally, some research has been extending the use of fire modeling tools to very practical and impactful topics such as the effect of ventilation strategies on firefighting outcomes (Kerber, 2010). One tactic for firefighters is to simply breakdown a door or a window to gain access or spray water. This action induces a rush of air into the compartment/building and could adversely change the fire dynamics especially in an under-ventilated situation. As such, the dangers associated with backdraft during firefighting operations are well known and are another area of study where CFD based fire modeling is contributing (Hwang & al., 2010).

TECHNICAL PLAN

The intention of this research is to assess and advance the applicability of HPC based tools, specifically CFD based fire modeling code FDS in predicting the behavior of compartment fires, when there is a combustible ceiling along with open ventilation. This report is part of a broader research effort to understand the fire performance of various wood structural support components in residential constructions.

As shown in Figure 6, the work in this research report, Task 8b, involves simulation of large-scale laboratory basement fire testing carried out in Task 6. However, the fire modeling will focus on simulating one particular scenario from the many that were tested. This single scenario consists of a basement fire developing under conditions of open ventilation and an unprotected engineered wood I-beam ceiling.

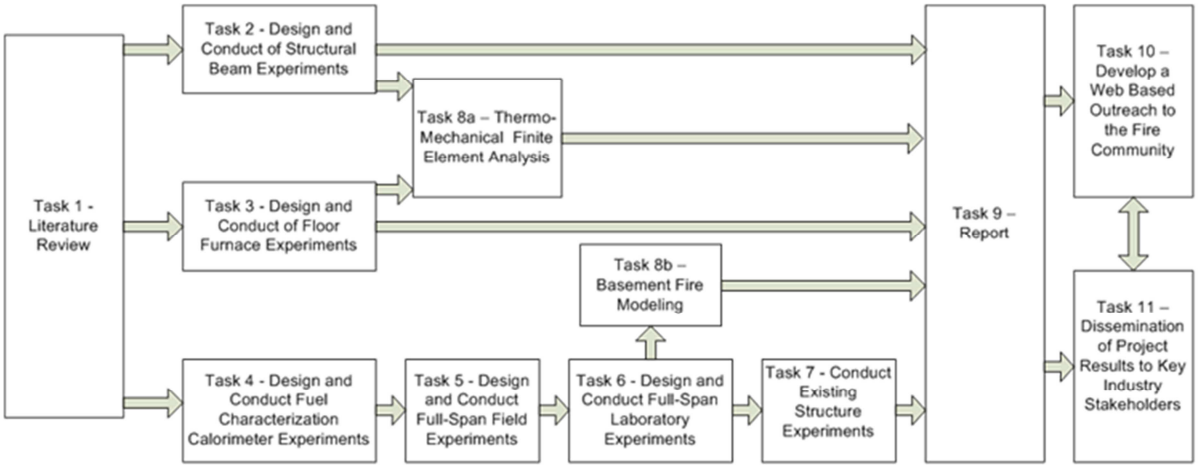

Figure 6 Overall Research Tasks

FIRE DYNAMICS SIMULATOR MODEL SETUP

One of several experiments conducted on a full-span laboratory basement structure was modeled (Kerber & et al., 2011). The structure is shown in Figure 7. It is a simple rectangular basement with several openings including a stairway. As seen in the photo, the basement ceiling (or first floor) was loaded with water filled barrels to help generate a specified design stress level. Since the modeling in this report is a CFD based fire model, there will only be predictions related to fire dynamics such as heat and mass transport. Research on the thermal-structural modeling of wood building components in fire was also a part of this overall project and is documented in a separate report (Tabaddor, 2011).

Figure 7 Photo of actual test basement structure

Basement Geometry and Mesh

The overall dimensions of the basement are shown in Figure 8[2]. There are basically 3 windows and 2 doors. The window is 81 cm (32") wide by 122 cm (4') tall. The door is 91 cm (3') wide and 206 cm (6'9") tall. Height of the basement is 284 cm (9'4"). There is a stairway with a sloped ceiling. The ceiling at the top of the staircase hallway is 243 cm (8') above the basement ceiling. The space

[2] For more information refer to the test report (Kerber & et al., 2011).

directly below the stairs is encased by walls so the underside is unexposed. The ceiling consists of a series of equally spaced I-joist beams supporting a wood subfloor. Each beam was approximately 30 cm (12") deep with chords that were 6.35 cm (2 ½") wide and 3.81 cm (1 ½") deep. The web consisted of 0.95 cm (3/8") thick oriented strand board.

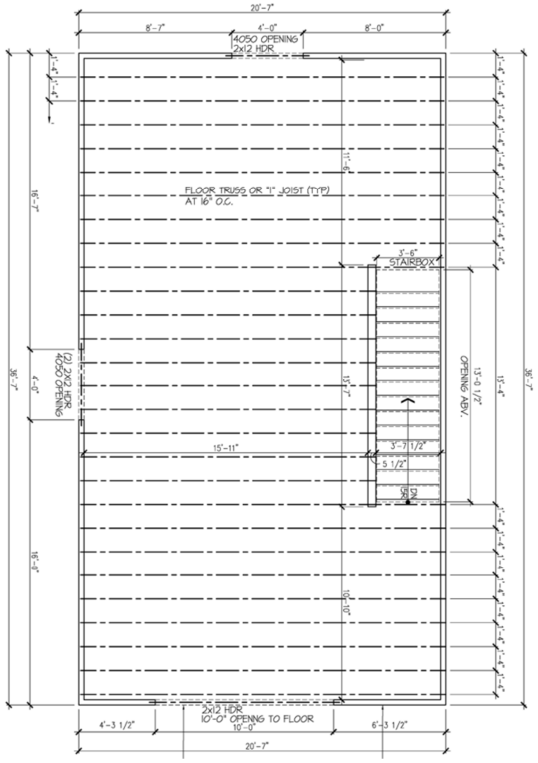

Figure 8 Drawing of basement structure

The details cited above were deemed important and so the basement model includes these features (Figure 9). One simplification was made for the I-joist. In FDS, it is much simpler to represent it as an equivalent rectangular cross section.

The overall computational domain included some open space beyond the basement structure so that air flow through openings would not need to be prescribed as boundary conditions and could be calculated as part of the entire response field. The outer box in Figure 9 indicates the boundaries of the computational domain.

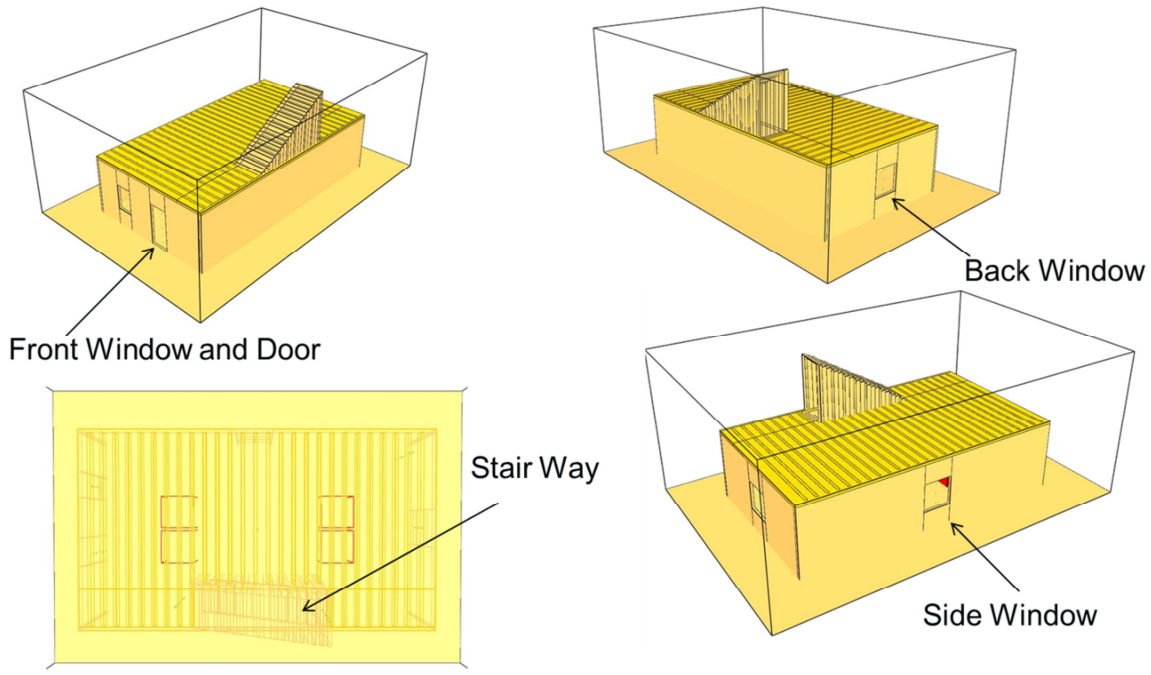

Figure 9 FDS model of basement structure

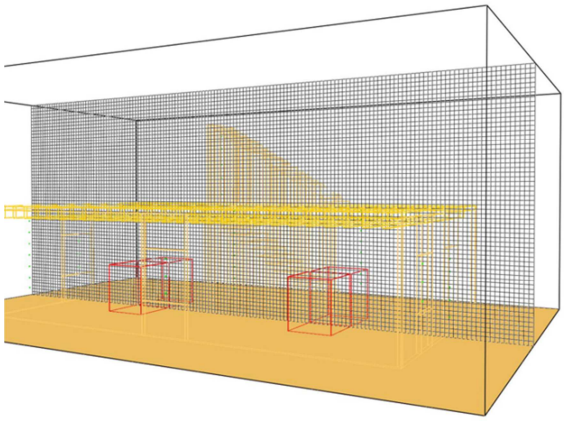

Figure 10 Image of grid plane within model

The computational domain was divided into cells measuring 10 cm x 10 cm x 10 cm for a total of 900,000 cells (Figure 10). The total number of cells determines both the accuracy and the total computational time. For the sloped ceiling of the stairway, FDS can only represent it through a series of staggered rectangular boxes or stair-stepping. This stair-stepping feature creates additional vorticity near the wall. FDS allows for some smoothing through a SAWTOOTH=.FALSE. command for each obstruction defining the stairway (McGrattan & et al., 2010).

Heat Source and Fuel Load

The initial heat source placed inside the basement during the test consisted of boxes filled with expanded polystyrene trays on top of pallets. Two sets of these box/pallet sets were placed with a 10 cm (4") space in between (Figure 11). Each wood/pallet measured 107 cm (42") on a side and had a height of 2 cm (5"). Each box measured 53 cm (21") on all sides. One stack consisted of 4 boxes on top of 6 pallets. Ignition was started from a point in the space between the two pallet/box sets at its base. Heat release rate (HRR) curves (Figure 12) were measured using a product calorimeter and some photos/videos of the burning process were recorded. The HRR curves for this heat source represent burning under conditions of full ventilation.

Figure 11 Photo of heat source

In FDS, an obstacle with the same overall dimensions of each stack of pallets and boxes was developed. In this case, the average experimental heat release rate curve (Figure 12) was entered as input (HRR per unit area) for the surfaces of the obstruction with some adjustments based on observations of actual fire burning characteristics. The HRR curve is not sufficient to uniquely define the burning of the pallet/box stacks. However, a review of the photos/videos from the burning of the pallet/box stacks during calorimeter measurements shows that the fire begins within the space of the two stacks burning mostly along these inner surfaces and then spreads to the top during the first 5 minutes after which the other sides are engulfed as the boxes burn from within (Figure 13). Since the total simulation time for this model will be no more than 5 minutes then the HRR during this time is mostly assigned to the facing and top surfaces of the box/pallet stacks with a small percentage assigned to the remaining faces. This detail will affect how the heat source radiates heat to adjoining

surfaces as the view factor will be different depending on which surfaces are burning and flame height.

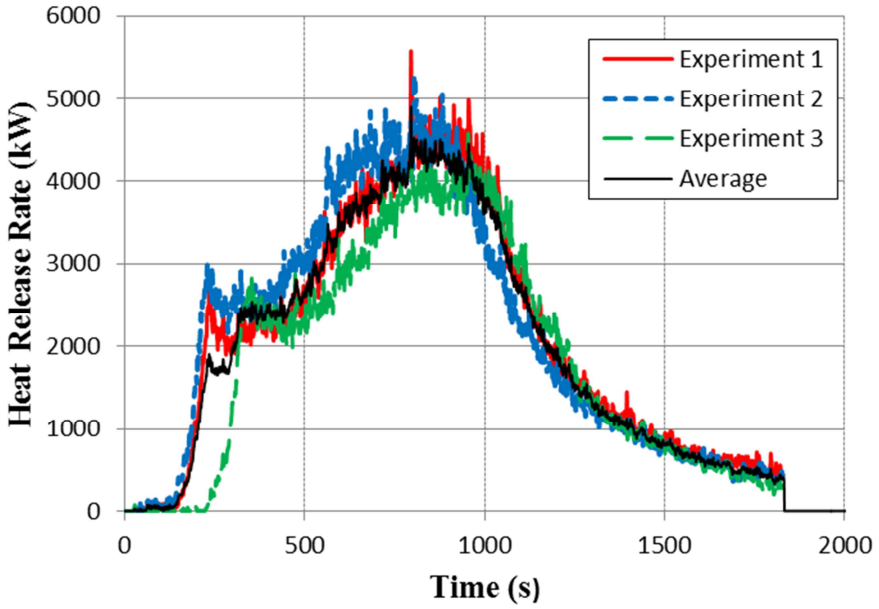

Figure 12 Experimental heat release rate curves used to define heat source

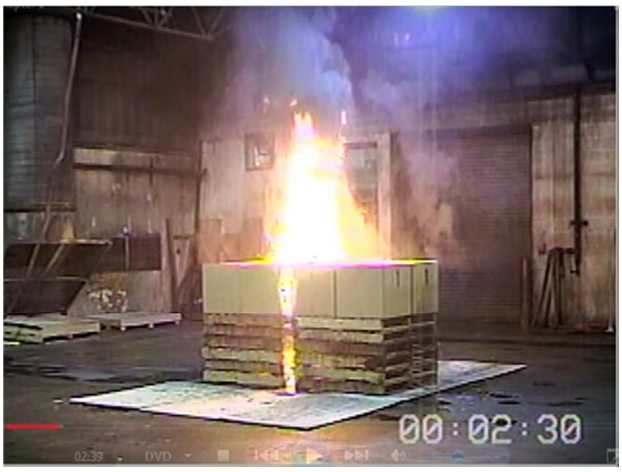

Figure 13 Photo of burning box/pallet stacks after 150s

The heat source, consisting of the 2 stacks of pallets/boxes, was placed near the basement door. This heat source was set to release heat upon start of the simulation. However, another set of 2 stacks of pallets/boxes were placed on the other side of the basement and are considered a fuel load (Figure 14) and also modeled as obstructions. In this case, the obstructions were assigned an ignition temperature of 300°C with the heat release rate profile uniformly assigned to the surfaces of the obstruction.

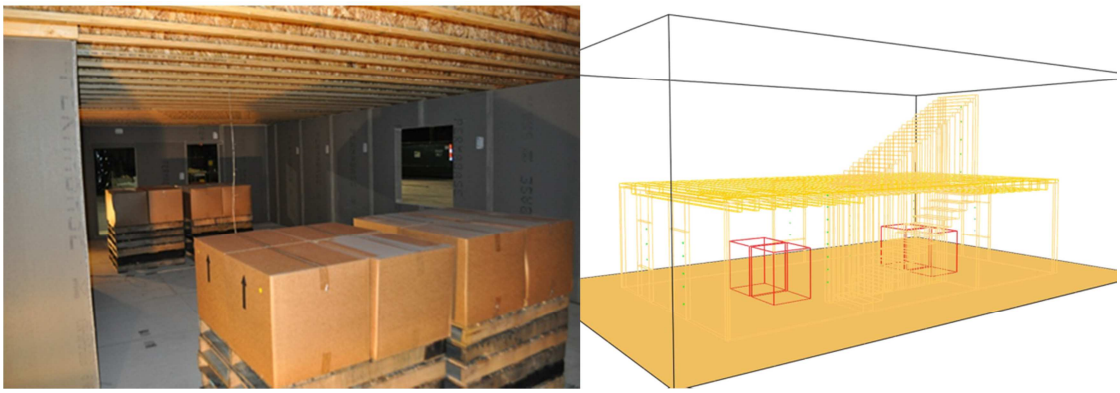

Figure 14 Picture of heat source and fuel load in both test (left) and model (right)

Thermal Properties and Boundary Conditions

The simulation was run with full ventilation, that is all windows and doors were open for the entirety of the calculation. An additional space outside of the building was included in the computational domain to help the accuracy of mass transport across the openings. In the test, the walls were sheathed with a base layer of 1.27 cm (½") gypsum board covered with a layer of 1.27 cm (½") of cement board. In this model, the basement walls and floor and the entire stairway were assumed to be inert and therefore prescribed as adiabatic.

Since the wood ceiling is directly above the fire source and is combustible, its thermal properties are a necessary input to the model. Furthermore, a simple representation of wood burning was selected based on heat release rate. In the model, once a cell reaches a critical temperature, the prescribed ignition temperature, it releases heat following a prescribed HRRPUA curve for the duration of the

simulation. For this model, the heat release rate was set to a constant value. The properties for wood were taken from Eurocodes (EN:1995-1-2, 2006) are listed below:

Specific heat: 1.3 kJ/kg °C

Thermal conductivity: 0.2 W/m °C

Density: 570 kg/m^3

Ignition temperature: 250 °C

HRRPUA: 150 kW/m^2

As noted previously, the computational domain extends beyond the structure so that boundary conditions need not be prescribed at openings such as windows and doors. The floor for the entire model was set to be a solid wall. For the other boundaries, an open vent condition was applied. For an open vent, it is assumed that ambient conditions exist beyond the boundary. As the analysis is transient, initial conditions must also be specified for temperature and airflow. In this case, the initial temperature is ambient and the air in the basement is still with some small noise introduced by FDS. Finally FDS v: 5.5.3 and revision number: 7031 was used for analyses presented in this report.

MODEL AND TEST RESULTS COMPARISON

In the test, speed and temperature measurements at discrete points at each opening, base of the stairs, center of room and one room corner were taken. Results from the model were extracted at the same locations. Along with these measurements, photos and videos of the flame and smoke growth and propagation were taken and will also be compared with visualization of flame from the model. Finally, taking the data analysis beyond what is available in testing, gas velocity and gas temperature contours throughout the domain will be examined for insight into the fire dynamics within the well ventilated basement with an unprotected wood ceiling.

Flame Dynamics

In this section, the main focus will be more on flame and heat generation than smoke. Figure 15 shows pictures from the test of the flames emanating from the openings within the basement. A similar set of flame visualizations from the model are also shown in Figure 16. For the model, very similar flaming is seen from all the openings; except that for the model, there is flaming through the back window which was not observed during the testing. One example of FDS's smoke generation and visualization output for the basement model is shown in Figure 17.

Figure 15 Pictures of flames through openings: front (left) stairway door at top (right)

Figure 16 Visualization of flames from openings of basement simulations

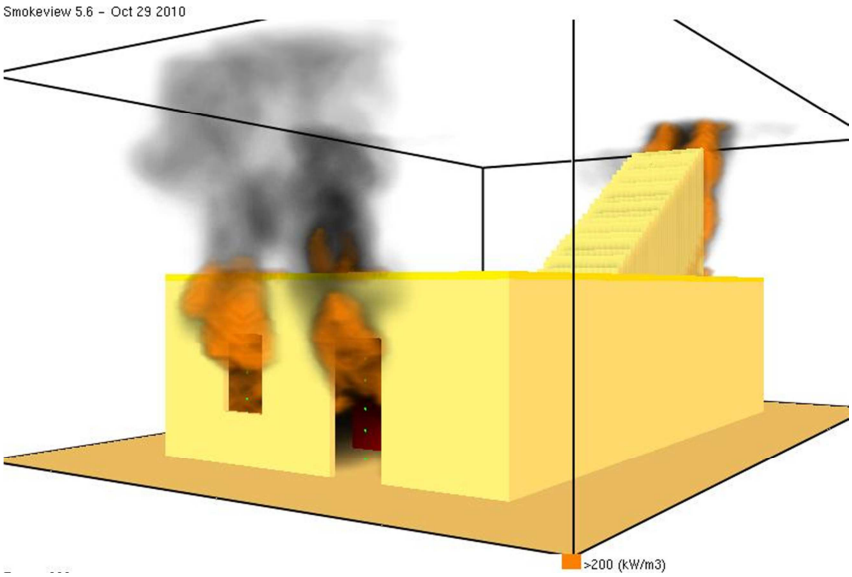

Figure 17 Visualization of smoke and flames from basement model

A post-test analysis of the video record of the fire suggests that the flames from the heat source attach to the wood ceiling above at approximately 140 s followed by sustained flaming through the first floor door from the hallway at 160 s. Figure 18 and Figure 19 show that for the model, initial burning of the wood begins around 165 s followed by sustained flaming through the first floor stairway door at 210 s. It is interesting to note how well the model predicts sustained flaming through an entirely noncombustible stairway and eventually through the open door, same as in the test.

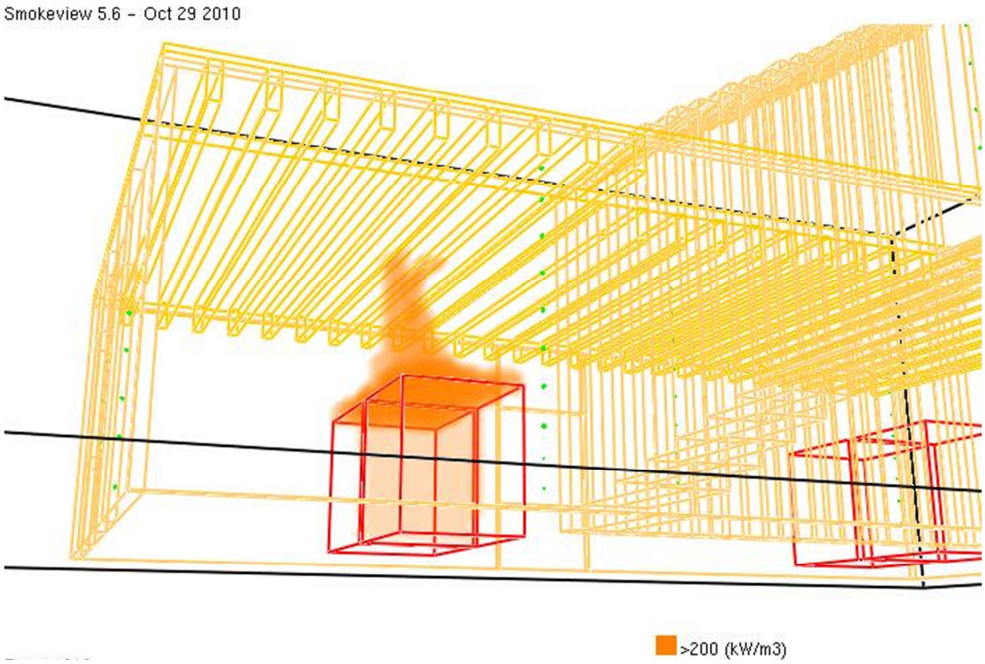

Figure 18 Visualization of flame from heat source at 165 s (basement door on left)

Figure 19 Visualization of flame through stairway at 210 s (basement door on left)

Figure 20 Video and IR camera records of basement fire test at 2:40 minutes

Figure 21 shows another interesting feature of the flame visualization in the model. The flames reach down into the middle of the basement. Looking at the upper left-most picture in Figure 20, the flames seen through the basement door are located halfway from the ceiling. In the window the flaming is less prominent.

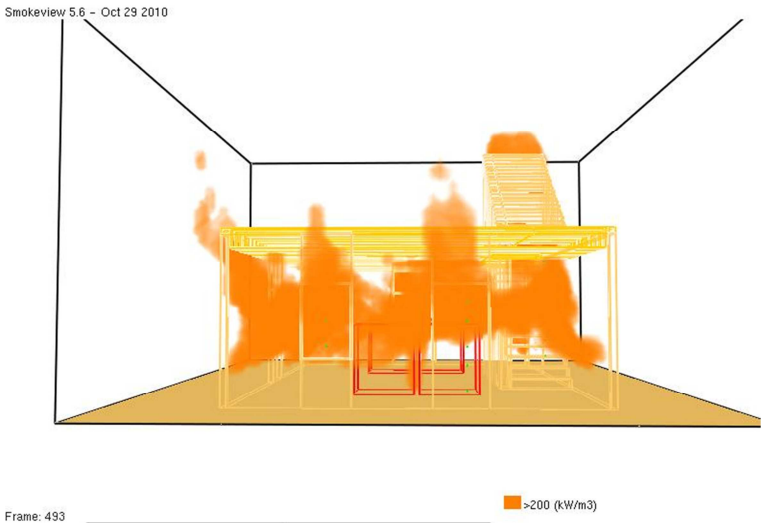

Figure 21 Frontal view of flame visualization within basement model (facing basement door)

In the model, it was noted that as time progressed, the flames began to occupy lower portions of the room. Figure 22 shows a comparison of the flames between the model (at 5 minutes – end of simulation) and the test (at 6 minutes where 2 of 4 video feeds were no longer available). Clearly flames can be seen to engulf the entirety of the space within the basement including the floor. The model is able to predict the same general flame behavior.

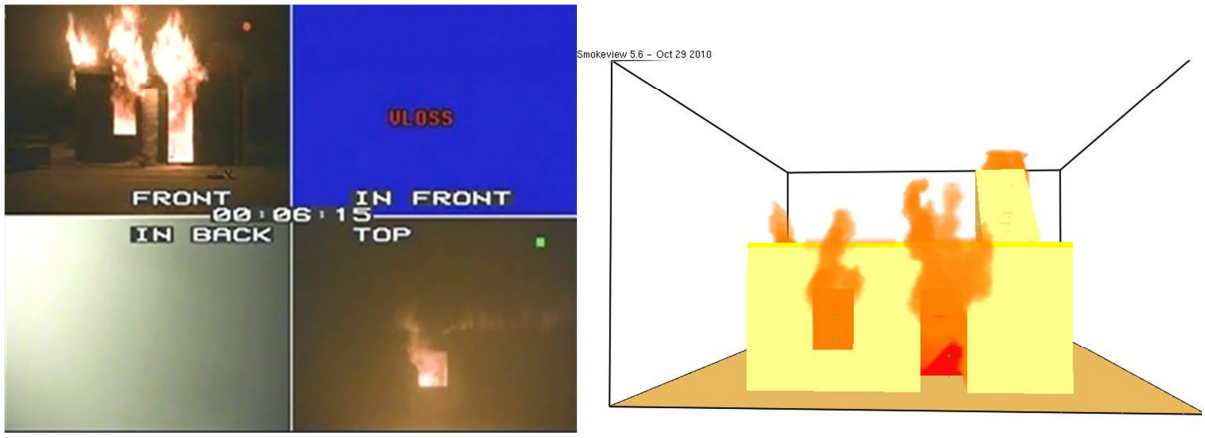

Figure 22 Comparison of flames towards end of test

In addition to the set of pallets and boxes used as a heat source, a similar set of pallets and boxes was placed on the opposite side of the basement representing a fuel load. Based on the video image, lower rightmost picture in Figure 20, that fuel load did not ignite as long as the video feed was available. In the model, this 2nd set of boxes and pallets never ignites for the duration of the simulation (300 s).

Temperature

Temperature measurements both within the basement compartment and at openings were recorded. For interior compartment temperatures, measurements were taken at 8 points along a vertical line at the center of the basement and at the corner between the back and side windows. This center point resides between the heat source and the other fuel load. The fuel load never ignites and so all the heat is generated by the heat source and burning of the wood ceiling. The corner point is located closer to the un-ignited fuel load than the heat source. When comparing with test temperatures, the model allows temperature output that matches more closely the operation of a thermocouple by including both convection and radiation heat transfer.

Figure 23 shows a comparison of the thermocouple temperatures for a point near the ceiling joists for the selected basement corner. For the model[3], the temperature rise is slower however after 100 s, the simulated temperatures rise higher than the experimental temperatures by 200°C. This same trend is observed for measurement points near the floor. This is certainly expected as the near wall/floor thermal boundary layer is dependent upon the flow boundary layer. In FDS, the boundary layer is not resolved for practical reasons and so it relies on an empirical model. However, the simulated temperatures begin to show better agreement for intermediate temperature measurements, away from any boundary, as shown in Figure 24. In the experiments, the temperature near the midair point is about 100°C higher after 150 s. For the model, this is also true after 150 s but the differences become less as the simulation reaches 300 s.

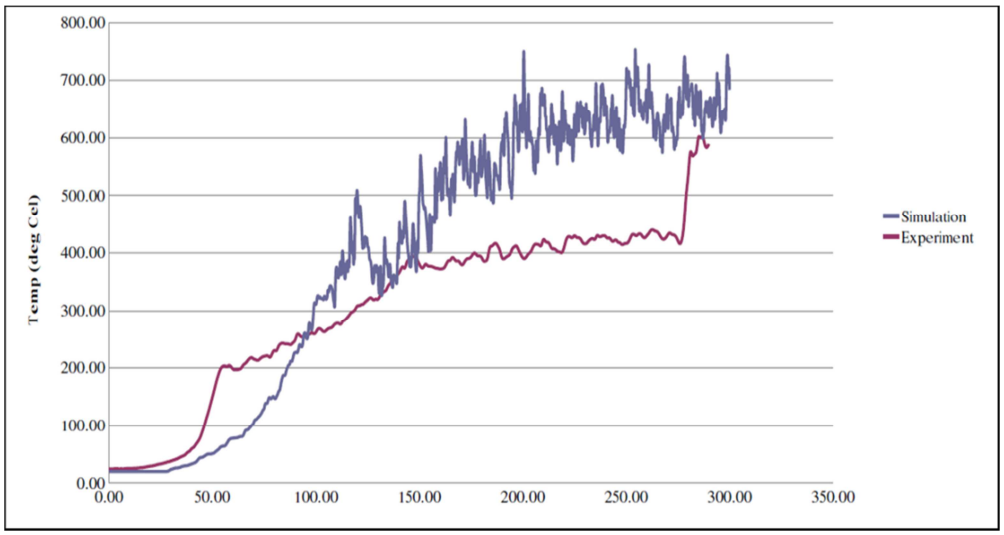

Figure 23 Temperature for corner of basement at point near the ceiling (TC1)

Figure 25 and Figure 26 show a comparison for the temperatures at the center of the basement for a point near the ceiling and in midair, respectively. For this central measurement of the basement temperatures, the model, after the first 100 s, matches the temperature measurements very well. The ability to model exactly the initial rise in heat and flame behavior is unreasonable at the level of resolution in this model both in terms of mesh but mostly due to some simplifying assumptions.

[3] For the model, temperature data was averaged so that 3 points per second are available similar to the data from the thermocouples.

However, the ability of the model to predict well the bulk temperatures after the first minute is very good. This data also shows that the temperatures within the center of the room are higher than that of the selected corner.

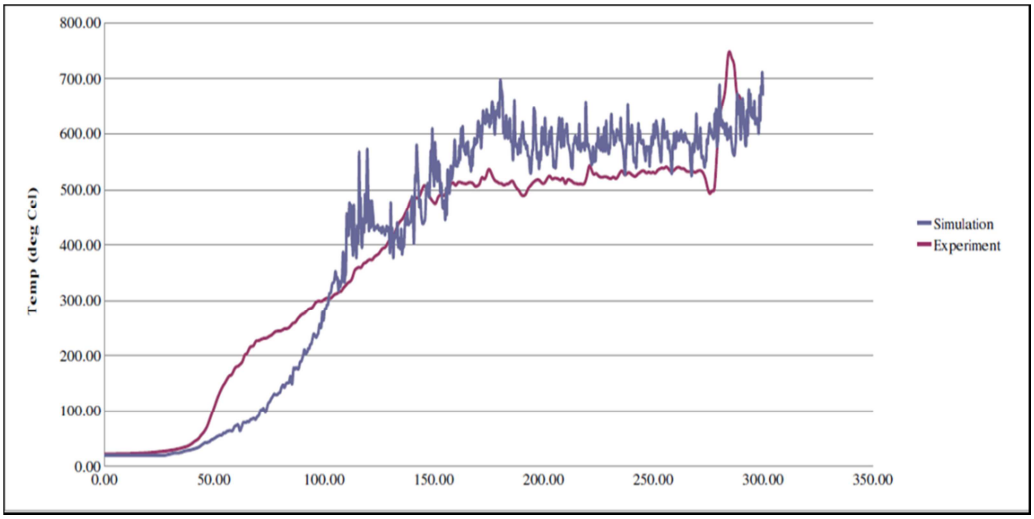

Figure 24 Temperature at the corner of the basement at a point in the midair (TC4)

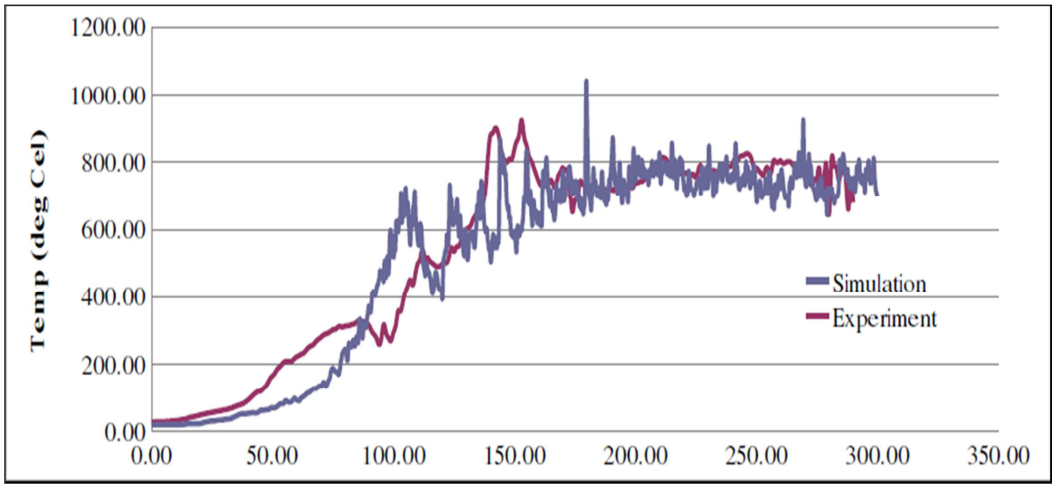

Figure 25 Temperature at center of the basement at a point near the ceiling (TC1)

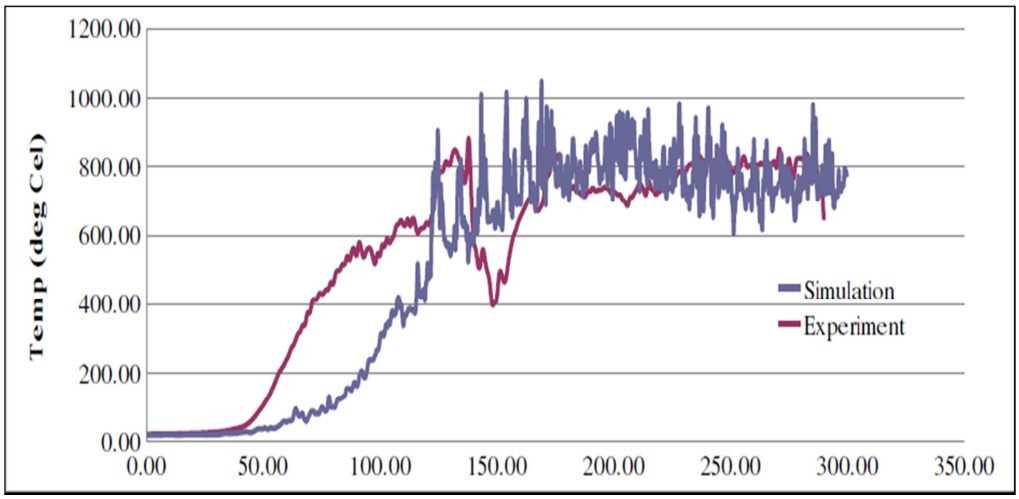

Figure 26 Temperature at center of basement at a point in midair (TC4)

Figure 27 and Figure 28 show temperatures at 2 points at the entry plane for the first floor door (or the door at the top of the stairway). For this opening, the model again lags the test data in temperature ramp-up during the first 50 s but thereafter provides a very good prediction of the temperatures.

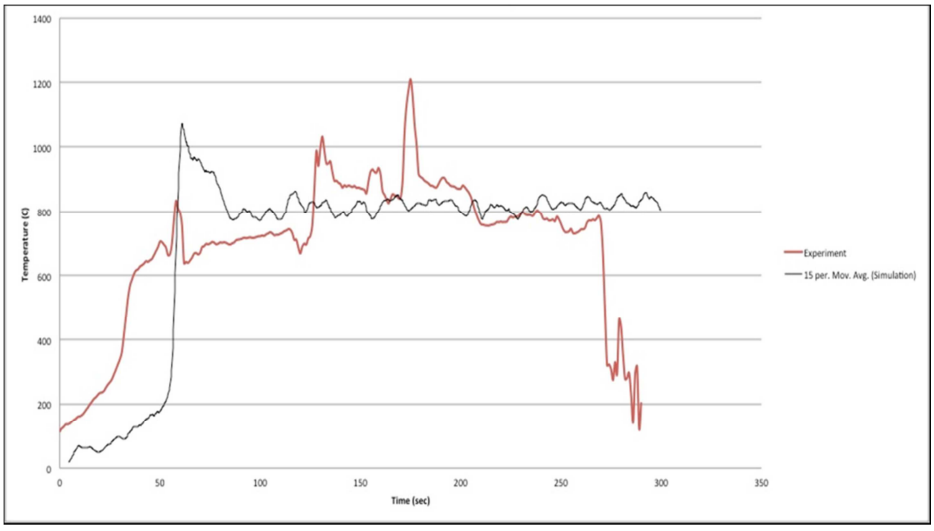

Figure 27 Temperatures at the first floor door at a point near the top of the door (TC1)

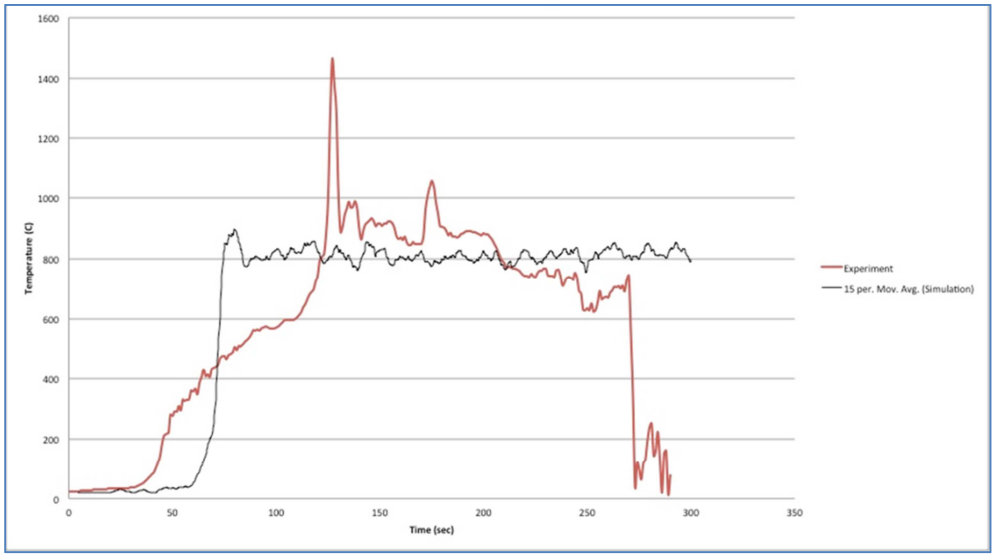

Figure 28 Temperatures at first floor door at a midpoint (TC4)

Figure 29 through Figure 31 show snapshots of the gas temperature contour at a cut that goes through the middle of the basement door. The growth of the hot gas layer is evident. By the end of the simulation, it is also apparent that the only cold region is air entering through the front door where the heat source (burning boxes/pallets) acts as a barrier to the entering ambient air.

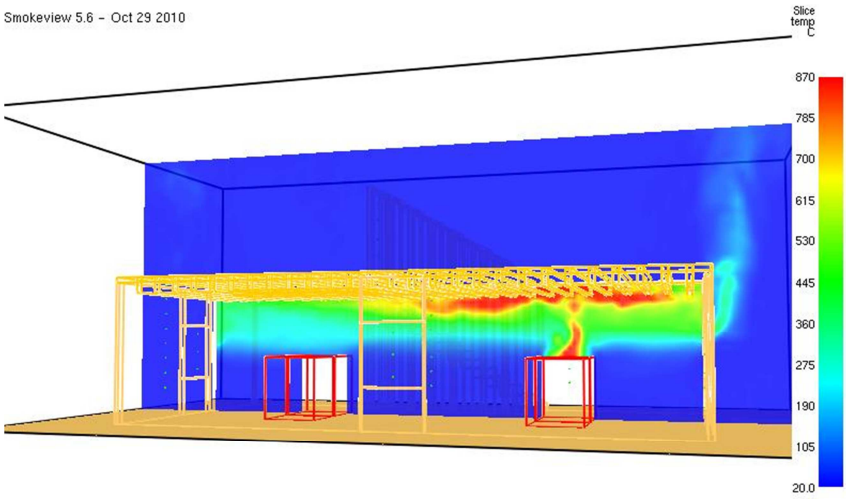

Figure 29 Temperature contours at 200 s (basement door on the right)

From the gas temperature contours, it is clear that ambient air is entering at a low temperature along the doorway floor. However, thermocouple measurements, shown previously, indicate a higher temperature as they include radiation effects.

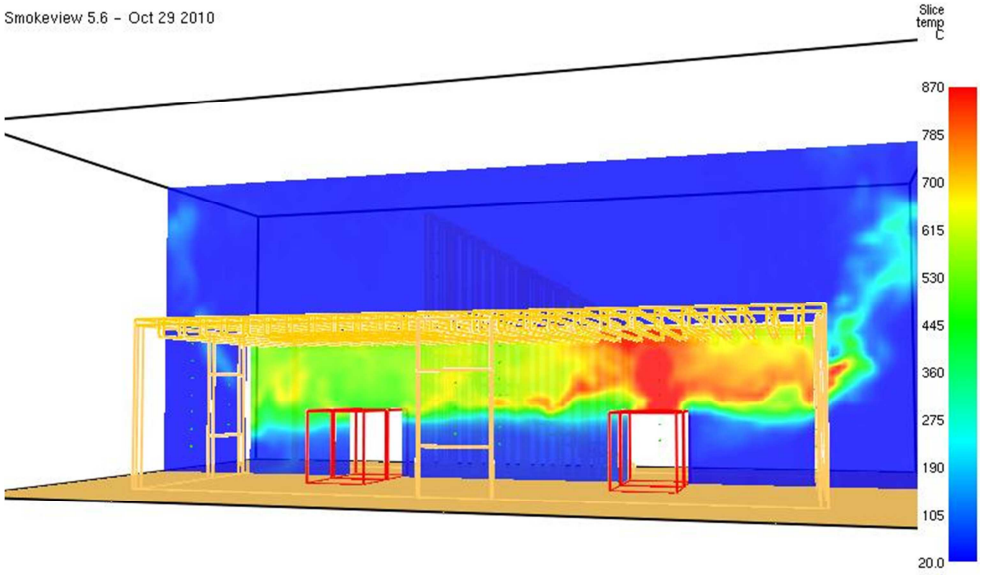

Figure 30 Temperature contour at 236 s (basement door on the right)

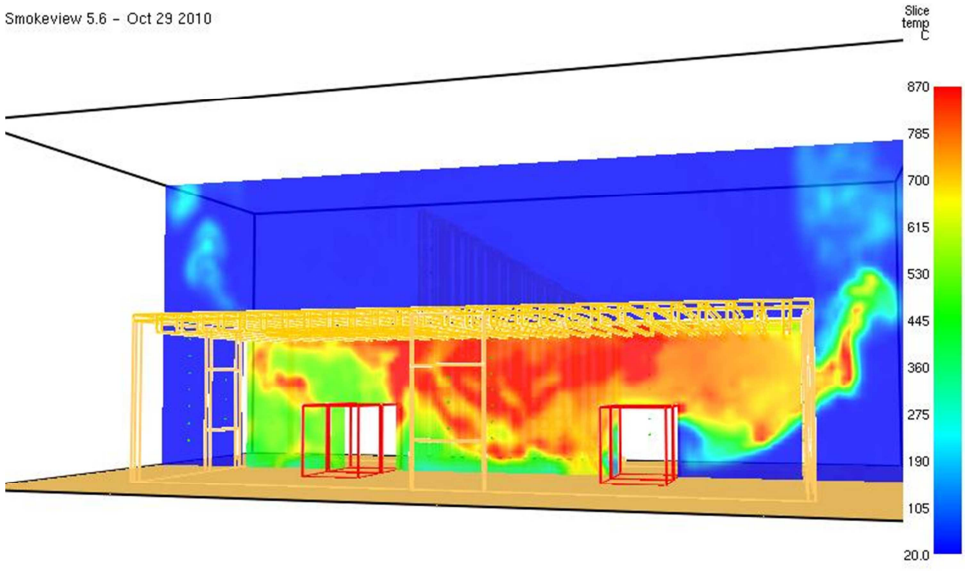

Figure 31 Temperature contour at 300 s

Figure 32 shows a snapshot of the gas temperature contours within the stairway. In this case, the hot gas layer does travel along the sloped ceiling with most of the stairway being heated above 100°C. The stairway door at the top is hotter than the door opening at the basement level.

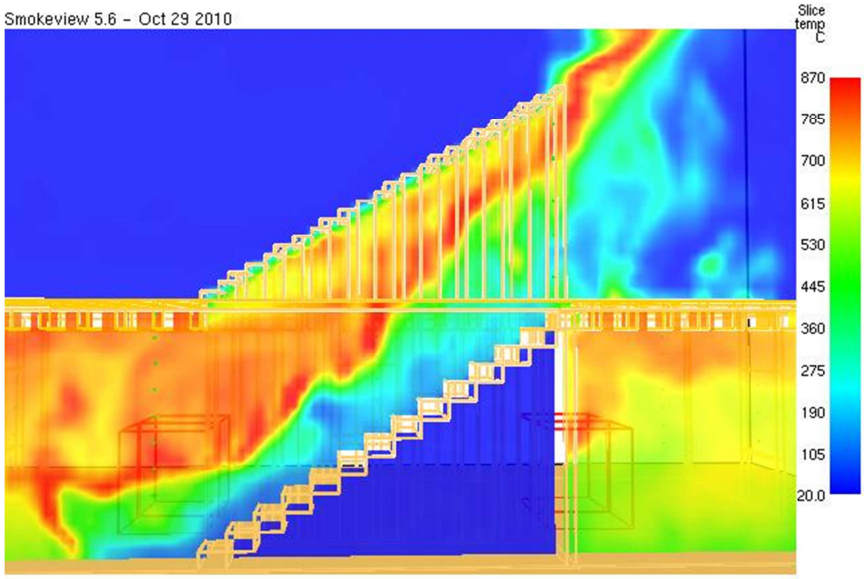

Figure 32 Gas temperature contours within stairway (in a plane though the middle)

Figure 33 shows another snapshot of the gas temperature contours, this time, through a plane parallel to the ceiling and below the bottom of the wood joist supporting the ceiling. There are 2 zones of high temperature apparent. This is a consequence of the hot air rising from the burning box/pallets and then running along the channels created by the parallel joist structure of the wood ceiling. One part of the flow heads towards the stairs and travels along the sloped ceiling of the stairway. One part travels towards the other end and then begins a path over the adjacent joists.

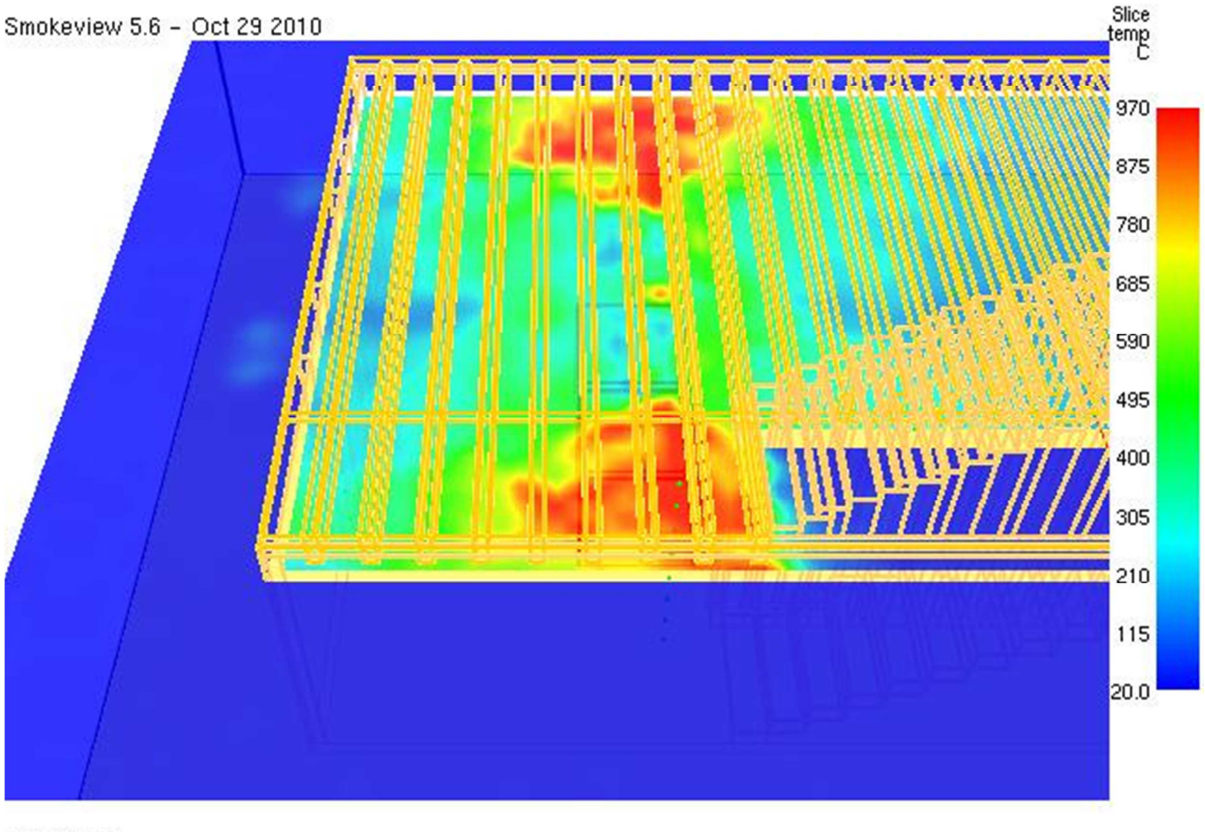

Figure 33 Gas temperature contours (in a plane parallel to the ceiling) just below the bottom of the joists

Velocity

A comparison the air velocity for the basement door is shown first. The results are shown for 3 of the 5 measurement points in the test. The first point is the top most point in the basement door (Figure 34). The speeds compare well and show that the flow is leaving (positive value indicates flow leaving basement) the basement compartment showing a peak eventually near 6 m/s for the test whereas the model predicts an earlier plateau reaching 4 m/s. Figure 35 shows the velocity measurements for a point in the middle of the basement door opening. In this case again, the agreement between model and test is very good. The negative values indicate that ambient air is entering the basement compartment. Finally, Figure 36 shows that air velocity entering near the bottom of the door is nearly as strong as that near the top of the door. Again, the model predicts quite well the velocity through this opening.

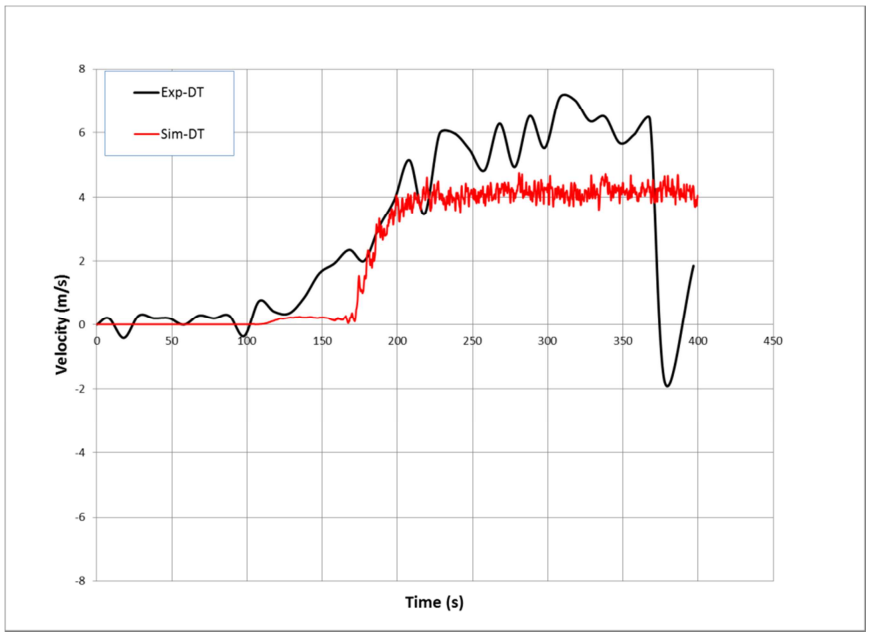

Figure 34 Velocity near the top of the basement door opening

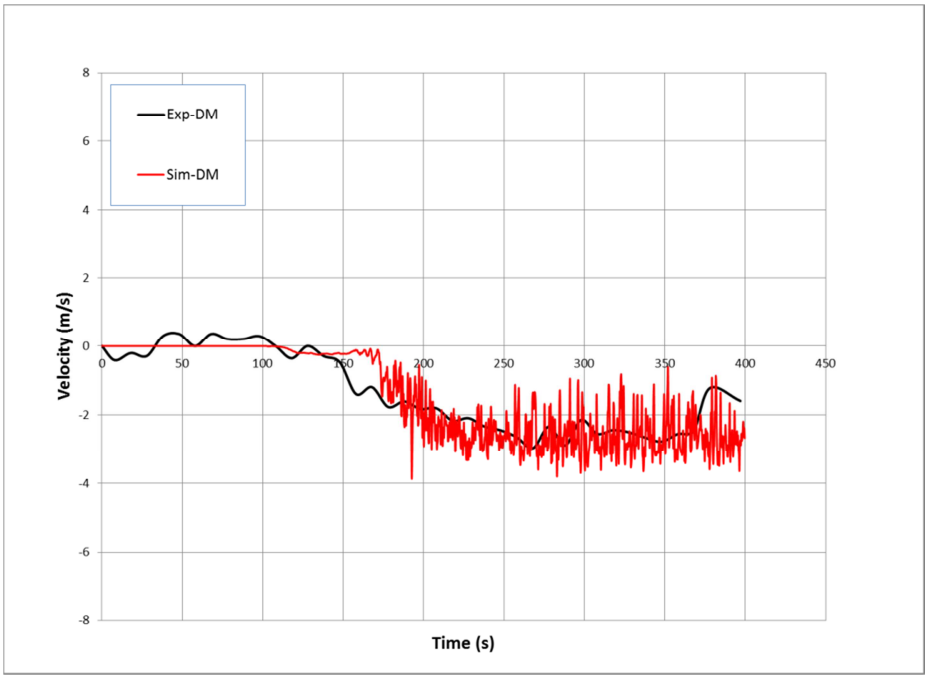

Figure 35 Velocity at midpoint of the basement door opening

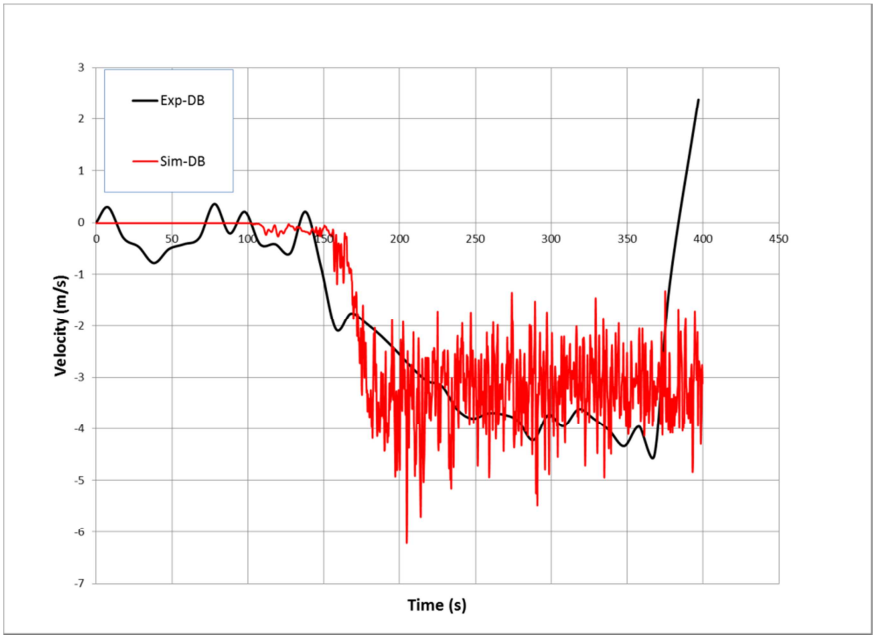

Figure 36 Velocity at the bottom point in the basement door opening

Figure 37 is an overlay of all the velocity measurements at the opening of the first floor door. In this case, all velocities are basically positive; suggesting that the air flow is mainly leaving the compartment through the stairway. Also the air speed through the basement is higher than that through the basement door reaching over 15 m/s. Overall, the model matches very well the test data at the opening of the first floor door. Similar plots are shown for all the windows in the appendix.

Next velocity contours are examined. With velocity contours, more detailed information on the flow regime is provided. Figure 38 shows a snapshot of the velocity contours along a plane passing through the middle of the basement door. There are clearly 2 recirculation zones visible due the presence and proximity of the box/pallet heat source to the basement door. As the ambient air rushes in, it impacts the side of the box/pallet set and recirculates immediately. In addition, another recirculation zone is visible above the box. In this case, as the air passing below the joists sees the effect of the wall and the previous recirculation zone, this creates a secondary recirculation zone.

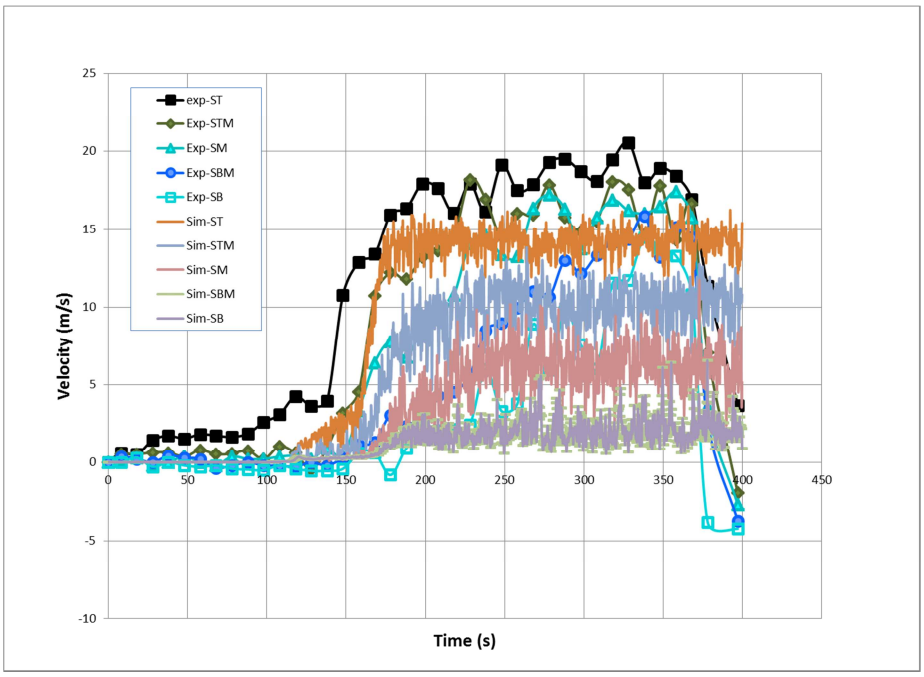

Figure 37 Velocity through the first floor door opening

Figure 38 Velocity contours at a plane intersecting the middle of the basement door

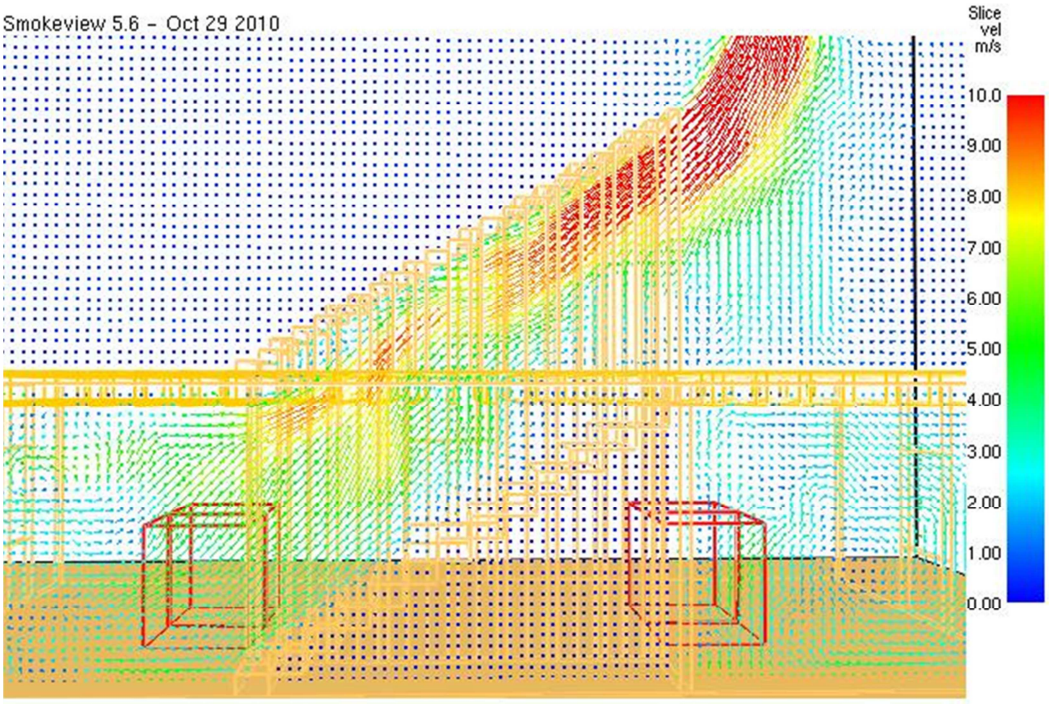

Figure 39 Velocity contours at a plane passing through the middle of the stairway

Figure 39 shows a snapshot of the velocity contours along the stairway. The strong flow along the top of the stairway is evident. A small recirculation zone before opening near the bottom of the stairs creates a non-monotonically changing velocity profile along the elevation in the early part of the stairway. Near the top opening, air is pulled in but quickly recirculates into the fast moving hot air above it.

Mesh Refinement

For the 10 cm mesh, the CPU time was on the order of 3 days on a state of the art computer using serial processing. As part of this research, the results from a model with a more refined mesh of 5 cm were also partially compared with the 10 cm mesh early in the investigation to assess the need for a very fine mesh. The increase in computational time was substantial, going from 3 days to over 3 weeks. Clearly, if such a refinement is not necessary to achieve reasonably accurate solutions within the basement compartment, then the entirety of the analysis could be carried out with the 10 cm mesh. Even though this analysis is presented last in this report, it was addressed early in the research

project. The following figures show that the difference between the 10 cm and 5 cm mesh were minimal at the selected points.

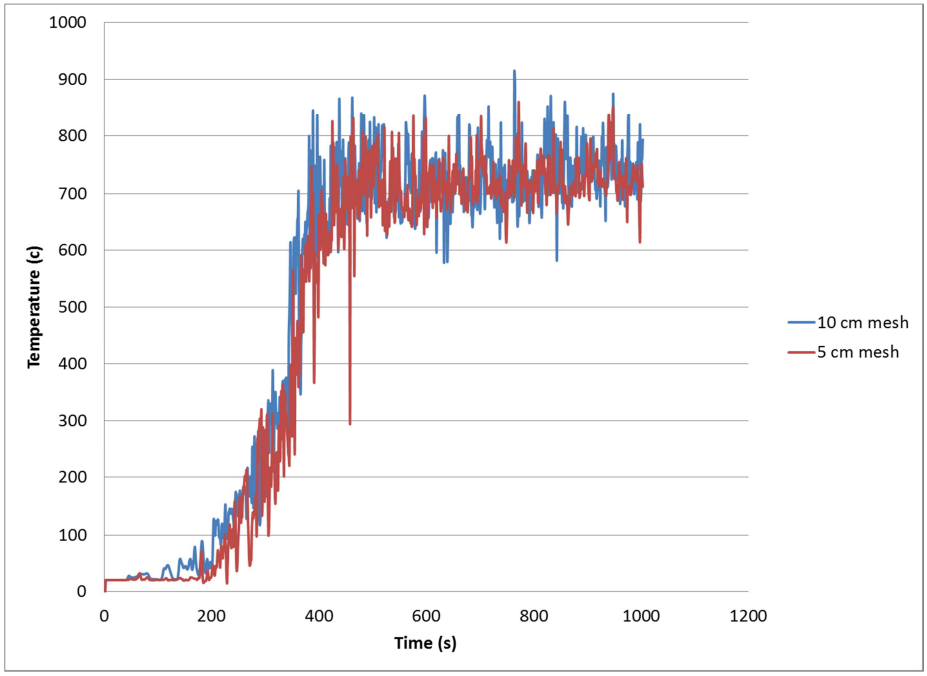

Figure 40 Comparison of thermocouple temperatures at the top of basement door

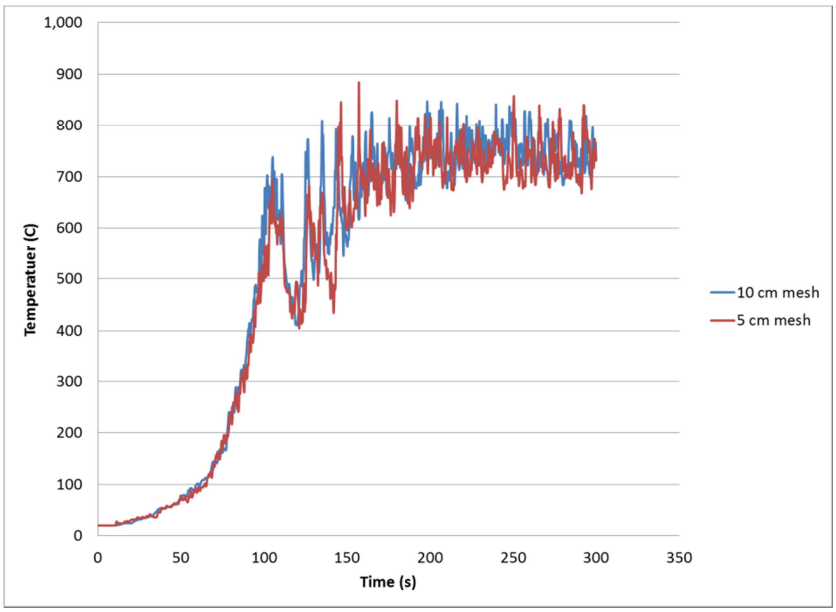

Figure 41 Comparison of thermocouple temperatures at the center of the room for the top position

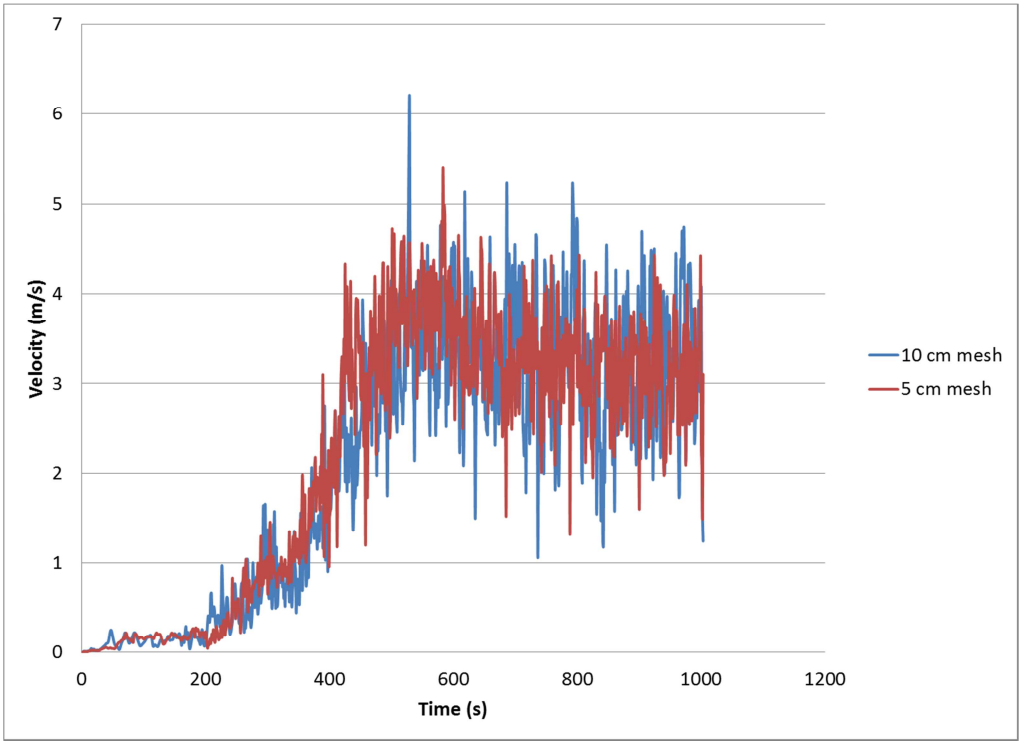

Figure 42 Comparison of velocity at the top of the basement door

SUMMARY OF FINDINGS AND RECOMMENDATIONS

This objective of this research was to help advance the use of HPC based tools, specifically FDS, in the field of fire engineering and science. The specific example concerned the fire dynamics within a basement with openings and an unprotected wood ceiling with geometric complexity.

The results in this study show that predicting the fire growth within basements with wood ceilings can be achieved reasonably well with FDS and that sensitivity analysis could be carried out, expanding this exercise to include some of the other experiments that were conducted as part of this overall research program. Results from the basement model appeared to compare well with discrete test measurements for temperature and velocity. The model did deviate in some instances quantitatively yet qualitative trends were very similar. In general, the bulk temperatures within the compartment were more accurate than those near openings. However some areas of improvement are noted below.

First and foremost, this exercise demonstrates the importance of accounting for the validation needs of modeling versus ordinary testing during the planning phase. For model validation, the selection of validation points is not always obvious. There are some guidelines such as measurements in regions where high gradients in key parameters are expected. For this basement, with the parallel joist configuration, the placement of velocity sensors would have been very helpful. This would have contributed data on the approach in FDS for modeling surface flows. In FDS, for an LES simulation, the boundary layer is not well resolved especially with only a few cells capturing the gap between the joists. This is expected to be a possible source of error for the flow between the parallel joists.

Since all the heat is generated by the box/pallets sets and the wood ceiling, both described by prescribing a heat release rate relationship, any inaccuracies would certainly have a big impact. For instance, for the heat release rate of wood, no profiles were readily available from published literature only single values.

For solids, the thermal conduction model is only 1-D and surfaces of the same obstacle do not communicate thermally. As such, FDS cannot account for burning through of the wood which is actually happening in this case. Since the joists were comprised of engineered wood I-beams, it is

known that for these beams, the thin webs burnout first, creating through holes for flames and air, eventually causing the lower chord to fall down. With an ability to model this aspect the air flow between the joists, the predictions will be less accurate especially in the region over the heat source as time progresses in the simulation.

WORKS CITED

Chen, C., & et al. (2010). Experimental Investigation and Numerical Simulation of a Furnished Office Fire. *Building and Environment*, 2735-2742.

Coyle, P., & et al. (2007). Further Validation of Fire Dynamics Simulator using Smoke Management Studies. *International Journal of Engineering Performance Based Fire Codes*, 7-30.

Dey, M. (2009). *Evaluation of Fire Models for Nuclear Plant Safety and Risk Analysis.* Deytec Inc.

Eliasson, J., & al., e. (2008). Enclosure Fires, Gravity Waves and the Backdraft Problem. *Journal of Fire Sciences*, 373-397.

EN:1995-1-2. (2006). *Eurocode 5: Design of Timber Structures.*

Floyd, J., & et al. (2005). A Network Fire Model for the Simulation of Fire Growth and Smoke Spread in Multiple Compartments with Complex Ventilation. *Journal of Fire Protection Engineering*, 199-231.

Gant, S. (2010). Reliability Issues of LES-Related Approaches in an Industrial Context. *Flow, Turbulence, and Combustion*, 325-335.

Guigay, G., & al., e. (2006). Numerical and Simple Engineering Approach to the Determination of Combustion Products in Strongly Under-Ventilated Fires Prior to Backdraft. *First Workshop on Fires in Enclosures.*

Hartin, E. (2009, September 17). Retrieved from Reading the Fire: Putting it all together: www.cbft-us.com

Hwang, C., & al., e. (2010). Studies on Fire Characteristics in Over and Underventilated Full-Scale Compartments. *Journal of Fire Sciences*, 459-486.

IStructE. (2007). *Guide to the Advanced Fire Engineering of Structures.* The Institution of Structural Engineers.

Karlsson, B., & et al. (2000). *Fire Enclosure Dynamics.* CRC Press.

Kayili, S. (2005). *CFD Simulation of Fire and Ventilation in Stations of Underground Transport Systems.* Middle East Technical University.

Kerber, S. (2010). *Impact of Ventilation on Fire Behavior in Legacy and Contemporary Residential Construction.* Underwriters Laboratories Inc.

Kerber, S., & et al. (2011). *Full Scale Floor System Field and Laboratory Fire Experiments.* Underwriters Laboratories Inc.

Lin, C., & et al. (2006). Ventilation Effect on Fire Smoke Transport in a Townhouse Building. *Heat Transfer - Asian Research*, 387-401.

Liu, Y., & et al. (2004). Comparison of CFD fire model Against a Venitlated Fire Experiment in an Enclosure. *International Journal of Ventilation*, 169-182.

McGrattan, K., & et al. (2005). *Federal Building and Fire Safety Investigation of the World Trade Center Disaster: Computer Simulation of the Fires in the World Trade Center.* NIST.

McGrattan, K., & et al. (2010). *Fire Dynamics Simulator User's Guide (version 5).* NIST.

Novozhilov, V. (2001). Computational Fluid Dynamics Modeling of Compartment Fires. *Progress in Energy and Combustion Science*, 611-666.

Prosser, B., & et al. (2010). Conducting a Fire Modeling Study. *13th United States/North American Mine Ventilation Symposium*, (pp. 365-370).

Ryder, N., & et al. (2004). Consequence Modeling Using the Fire Dynamics Simulator. *Journal of Hazardous Materials*, 149-154.

Saunders, J. (2010). *The Prediction of Smoke Detector Activation Times in a Two-Storey House Fire Through CFD Modeling.* University of Canterbury.

Stroup, D., & et al. (2011). *Nuclear Power Plant Fire Modeling Application Guide.* U.S. Nuclear Regulatory Commission.

Tabaddor, M. (2011). *Modeling the Thermal and Structural Behavior of Wood Beams in a Fire Environment.* Underwriters Laboratories Inc.

Tabaddor, M., & et al. (2011). Complex Spray Pattern Measurements for Fire Sprinkler Modeling. *Suppression, Detection and Signaling Research and Applications.* The Fire Protection Research Association.

Yung, D. (2008). *Principles of Fire Risk Assessment in Buildings.* Wiley.

APPENDIX A

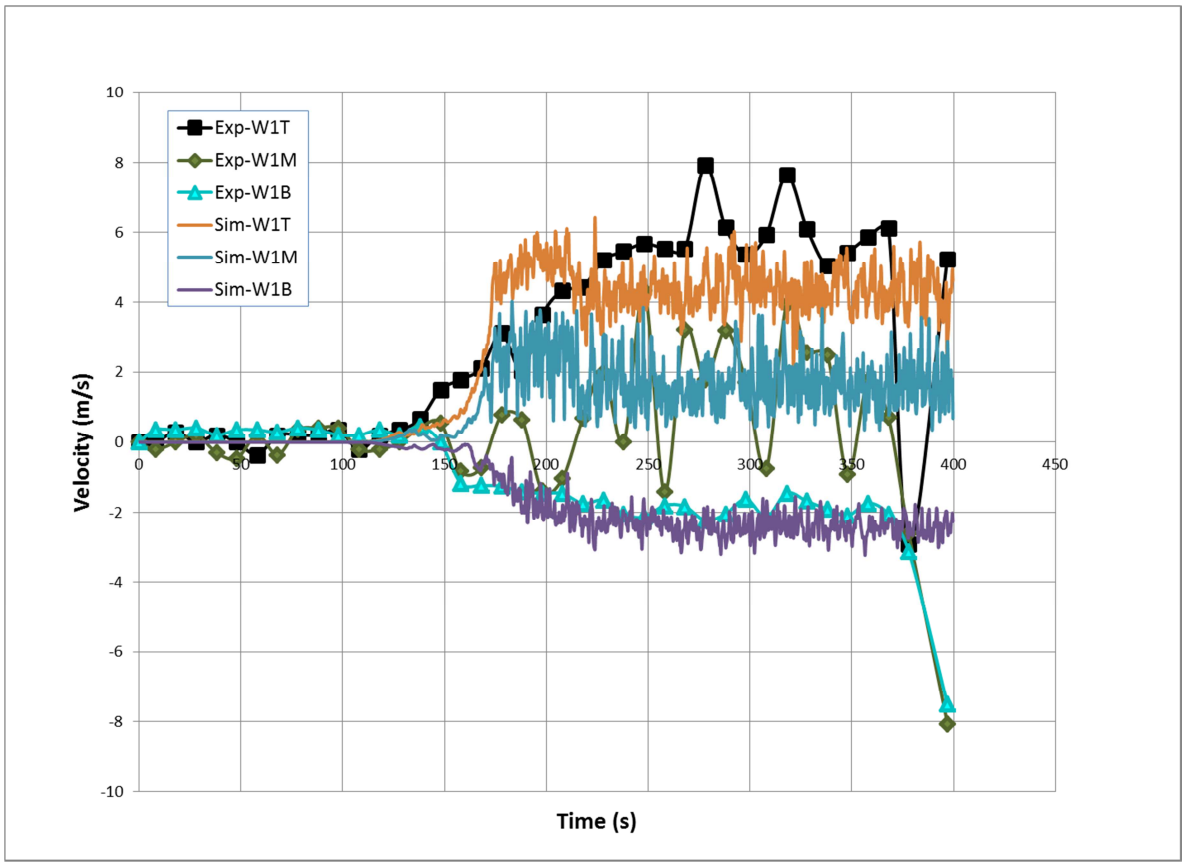

Figure 43 Overlay of velocities at front window

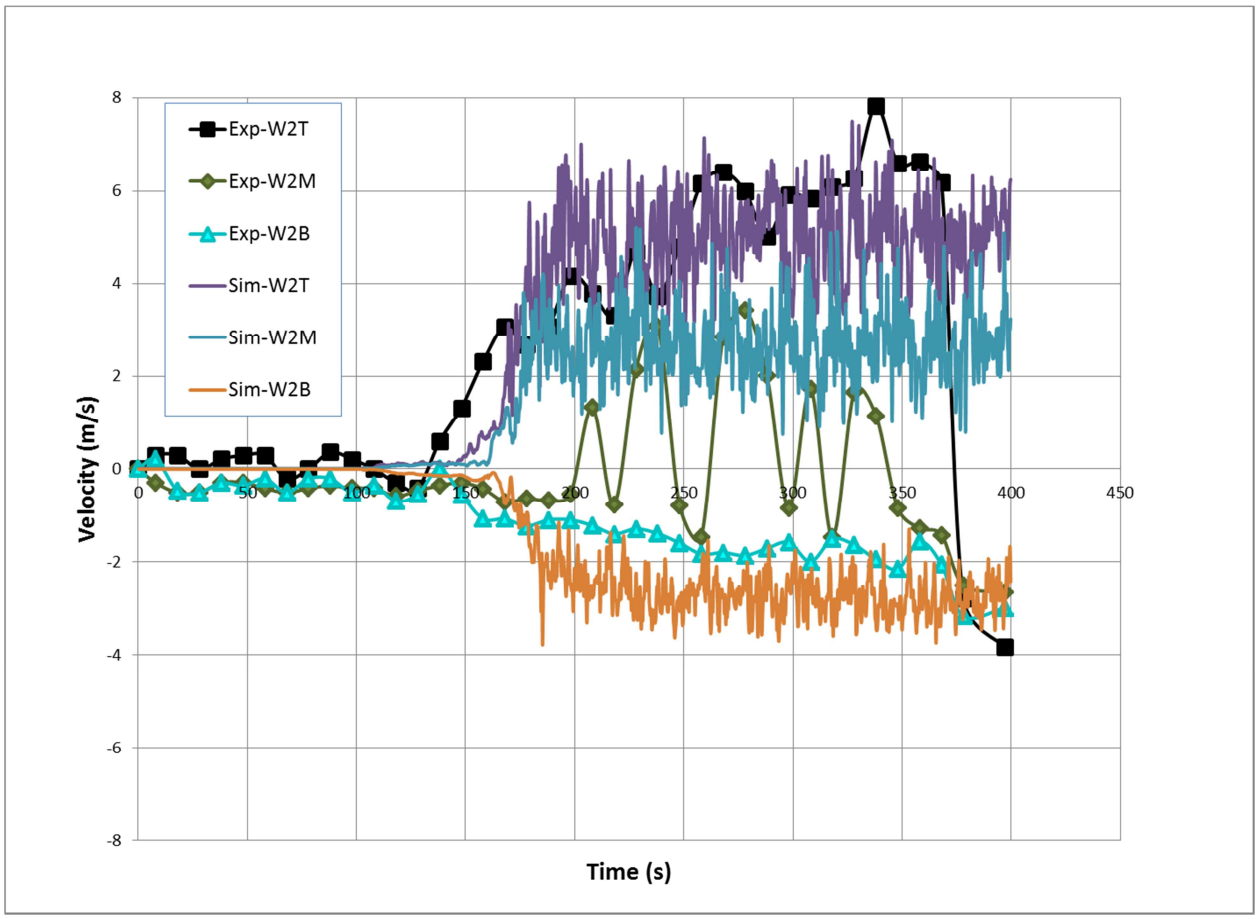

Figure 44 Overlay of temperatures at side window

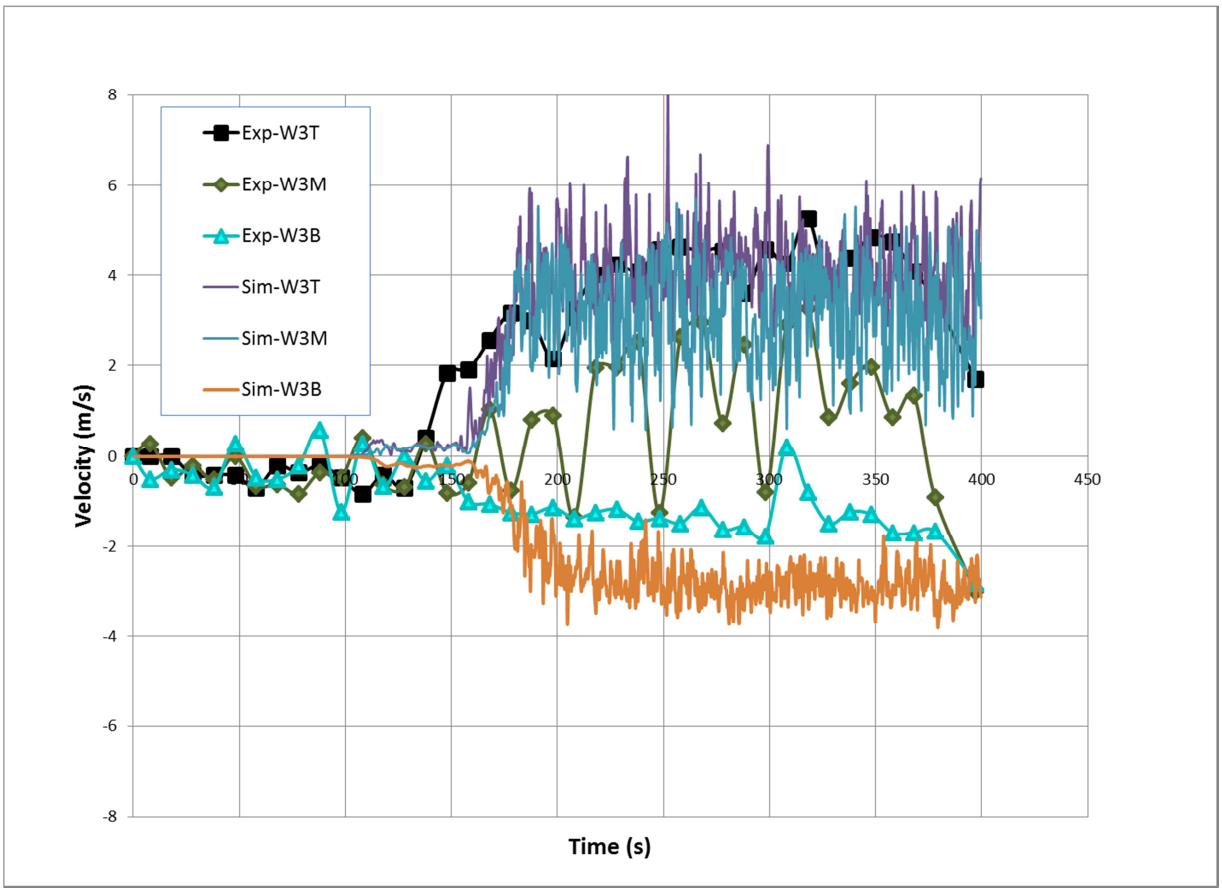

Figure 45 Overlay of temperatures at back window